



Department of Structural Engineering - Politecnico di Milano

GeoELSE2D User Guide for plane wave propagation

Web site: <http://geoelse.stru.polimi.it/>

prepared by:

Chiara Smerzini

May, 2011

Contributors

Politecnico di Milano, Department of Structural Engineering

Roberto Paolucci, Chiara Smerzini

Munich RE

Marco Stupazzini

CONTENTS

CONTENTS	i
LIST OF FIGURES	iii
LIST OF TABLES	v
1. THE DOMAIN REDUCTION METHOD AS AN EFFECTIVE TOOL FOR PLANE WAVE PROPAGATION	1
1.1 THE DOMAIN REDUCTION METHOD (DRM)	1
1.2 THE DRM FOR PLANE WAVE PROPAGATION	3
1.2.1 Plane waves as a distribution of body forces	3
1.2.2 Plane waves as an effective seismic excitation	4
1.3 VALIDATIONS	7
1.4 ACCOUNTING FOR BI-DIRECTIONAL SEISMIC INPUT	10
2. INPUT FILES FOR PLANE WAVE PROPAGATION ANALYSES	17
2.1 GENERATION OF THE SE MESH WITH CUBIT SOFTWARE	17
2.1.1 General criteria for spatial discretization	19
2.2 PRELIMINARY ANALYSIS FOR THE COMPUTATION OF THE EFFECTIVE DRM NODES	21
2.3 COMPUTATION OF THE EFFECTIVE FORCES: MATLAB INTERFACE PROGRAM	21
2.4 2D SIMULATION OF REDUCED PROBLEM BY GEOELSE	25
2.5 COMPUTATION OF THE SEISMIC RESPONSE UNDER BI-DIRECTIONAL PLANE WAVES	28
REFERENCES	31

LIST OF FIGURES

Figure 1.1 Modular two-step procedure named Domain Reduction Method (DRM)	2
Figure 1.2 Sketch of the method proposed for plane wave propagation analyses by GeoELSE	5
Figure 1.3 2D reduced model used as validation for plane wave propagation analyses by GeoELSE	8
Figure 1.4 Comparison between the numerical results by GeoELSE (black line) and the analytical solution (dashed grey line) for the model in Figure 1.3.	9
Figure 1.5 2D geological structure consisting of one soft layer over halfspace: validation of the code for a seismic input represented by plane P waves with angle of incidence $\gamma = 0^\circ$ and $\gamma = 20^\circ$	10
Figure 1.6 Comparison between the numerical results by GeoELSE (black line) and the analytical solution (dashed grey line) for the model in Figure 1.5.	11
Figure 1.7 Comparison between the DRM-based method and the standard single step approach for plane wave propagation analyses.	12
Figure 1.8 Circular valley under vertical plane SV waves: comparison between the DRM-based method (black line) and the standard single step approach (dashed red line) for plane wave propagation analyses.	13
Figure 1.9 Procedure for the evaluation of the seismic response of a localized irregular structure under bi-directional plane wave seismic input.	15
Figure 2.1 Flowchart with the main steps for the application of plane wave propagation analyses (DRM-based approach).	18
Figure 2.2 Example of 2D spectral element mesh for an idealized geological model, consisting of an alluvial basin in an elastic halfspace.	20
Figure 2.3 Example of <i>matfile.mat</i> file for plane wave propagation analysis (GeoELSE simulation with option SDRM = 3).	22

Figure 2.4 Example of <i>else2_input.d</i> file for plane wave propagation analysis (GeoELSE simulation with option SDRM = 3).	22
Figure 2.5 Computation of the list of effective DRM nodes.	24
Figure 2.6 Example of file <i>plane.ini</i>	25
Figure 2.7 Procedure to define a reference 1D soil profile for the computation of the free field solution under plane wave input.	26
Figure 2.8 Example of <i>matfile.mat</i> for GeoELSE simulation with SDRM = 2 (step II of DRM procedure) for plane wave propagation.	26
Figure 2.9 Example of <i>else2_input.d</i> for GeoELSE simulation with SDRM = 2.	27

LIST OF TABLES

Table 2.1	Description of file <i>plane.ini</i> .	25
Table 2.2	Description of file <i>H2d_convol.ini</i> .	29

1. The Domain Reduction Method as an effective tool for plane wave propagation

1.1 THE DOMAIN REDUCTION METHOD (DRM)

In the traditional numerical approach for seismic wave propagation analyses, the simulation is carried out by using a single model that includes the whole geological structure from the seismogenic source into the localized irregular region, including site effects or soil-structure interaction. The single-step approach is suitable for many engineering applications, especially when the causative fault is close to the region at study and the differences between the length of elements near the seismic source and of those representing the localized region do not exceed one order of magnitude. On the other hand, if the source is far from the region of interest or the scale of elements varies significantly from tens of kilometers to tens of meters, the computation cost becomes too large and the method becomes ineffective.

The Domain Reduction Method, referred to hereinafter as DRM, is a powerful *substructuring* technique which allows to overcome these computational problems. Dating back to the pioneering studies by [Herrera and Bielak \(1977\)](#), [Bielak and Christiano \(1984\)](#) and [Loukakis \(1988\)](#), several *substructuring* procedures were proposed making use of combinations of different computational methods: i) discrete wavenumber method + FDM ([Zahradník and Moczo, 1996](#)); ii) modal summation method + FDM ([Fah et al., 1994](#)); iii) FEM + BEM ([Bielak et al., 1991; Mita and Luco, 1987](#)); v) FE +FE ([Bielak et al., 2003; Yoshimura et al., 2003](#)); v) FD + FD ([Oprsal and Zahradník, 2002](#)).

The DRM essentially consists in subdividing the original problem in two subsequent models, as sketched in Figure 1.1. Starting from the original problem (Step 0 in Figure 1.1), in a first step (auxiliary problem) one considers a background geological model, where the geological feature of interest has been removed and replaced by the same materials of the surrounding soil, and computes the corresponding free-field ground motion in the halfspace due to the prescribed seismic source. The term free-field motion denotes the ground motion obtained in absence of the localized irregular feature under study. The numerical grid used at this stage is generally fairly coarse and the element size is controlled by the softest material in the background model (exterior domain in Figure 1.1). Note that, unless the seismic excitation remains unchanged, simulation of the auxiliary problem needs to be performed only once, even when some features or system parameters of the localized structure are supposed to

vary.

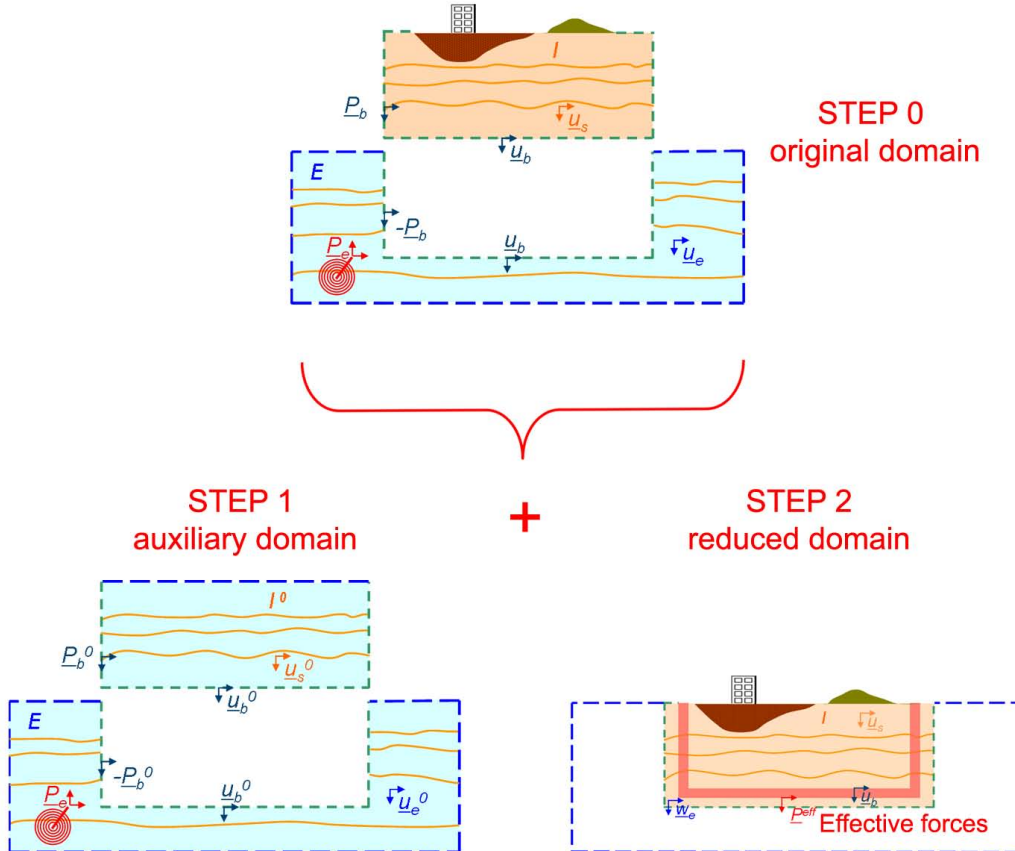


Figure 1.1. Modular two-step procedure named Domain Reduction Method (DRM). The original problem (Step 0, top panel) of seismic wave propagation from a seismic source to irregular localized structures is *substructured* into two numerical submodels (Steps 1 and 2, bottom panel). Step 1 (left bottom panel): auxiliary model including the seismic source and propagation path in earth media but without the localized structure (exterior domain). Step 2 (right bottom panel): reduced model including the localized geological structure(s) of interest (interior domain). Coupling of Step 1 and 2 is given by a set of effective forces, computed from the free-field solution (auxiliary problem) and applied within a strip of spectral elements as an equivalent dynamic excitation.

In a second step (reduced problem), one focuses on a reduced numerical model, discretized to the desired accuracy, which contains the geological feature (e.g. basin or topographic irregularity) and excludes the seismic source and most of the propagation path from source to site. Note that the reduced model is only slightly larger than the geological feature itself so that the computational grid can be easily optimized with respect to the original problem. The size of the elements of the reduced model may vary from a few kilometers down to a

few meters/centimeters, depending on the feature of interest. Seismic excitation is introduced in the reduced problem in the form of localized effective forces computed from the free-field displacement and applied within a single-element fictitious interface that separates the exterior domain from the interior one, as highlighted in Figure 1.1. The effective forces act as an equivalent dynamic excitation.

The main advantage of this modular two-step procedure is the possibility of computing the free-field displacements and, consequently, the effective forces, by either numerical or analytical methods suitable for simplified geological configurations (e.g. horizontally layered crustal model) and arbitrary seismic excitations (point/extended source or plane wave propagation).

1.2 THE DRM FOR PLANE WAVE PROPAGATION

A new procedure was recently proposed to perform seismic wave propagation analyses in arbitrarily complex geological structures, including possible SSI effects, subject to the incidence of plane waves with arbitrary angle of incidence, exploiting the advantages of the DRM. After illustrating the basic features of plane wave source implementation in the previous version of the code (plane waves as distribution of forces), we will describe the approach followed for coupling the DRM with analytical methods for plane wave propagation.

1.2.1 Plane waves as a distribution of body forces

In the previous version of GeoELSE, the plane wave source was implemented as a distribution of forces along the wavefront, computed in such a way to impose a given displacement time history $\tilde{u}(t)$. It can be proved that this can be efficiently obtained by adding to the equilibrium equation an external force term, proportional to the time derivative of the imposed displacement.

Following Faccioli et al. (1997), let us consider the 1D wave propagation equation:

$$\rho \frac{\partial^2 u}{\partial t^2} = (\lambda + 2\mu) \frac{\partial^2 u}{\partial x^2} + f(x, t) \quad (1.1)$$

where λ and μ are the Lamè coefficients and $f(x, t)$ is an equivalent uniform body force distribution for a vertically propagating displacement plane wavefront time dependence $\tilde{u}(t)$. In a 3D infinite homogeneous medium, the displacement in the i direction, generated by an uniform distribution of body forces $\underline{f}(x, t) = \phi(t)\delta(x - x_0)\underline{e}_i$ acting on the plane $x = x_0$, is given by:

$$u(x, t) = \frac{1}{2\rho V_S} H\left(t - \frac{|x - x_0|}{V_S}\right) \int_0^{(t - \frac{|x - x_0|}{V_S})} \phi(\tau) d\tau \quad (1.2)$$

where $H(\cdot)$ is the step function, ρ is the soil mass density, V_S is the S-wave propagation velocity and $\delta(x)$ is the spatial Dirac delta.

Therefore, the time dependence of the force distribution ϕ is obtained by differentiating Eq. 1.2 with respect to time and evaluating the result at $x = x_0$ (Graff, 1975), leading to:

$$\phi(t) = 2\rho V_S \frac{\partial \tilde{u}}{\partial t} \quad (1.3)$$

These equivalent body forces are applied to a particular set of nodal points located along an horizontal grid line near the bottom boundary of the numerical model. Specifically, the nodal points must lie inside a horizontal layer of quadrilaterals (in 2D) or hexahedral (3D) elements with constant height \tilde{L}_x . The reason for this is that the numerical approximation aims at resembling the 1D plane wave propagation of Eq. 1.1, hence the geometry must be constant along the x direction.

Such an approach presents two major drawbacks:

- it is not applicable to oblique plane wave propagation, unless the free-surface is rotated;
- wave propagation is badly affected by the absorbing lateral boundaries, the effectiveness of which is minimum for lateral incidence.

1.2.2 Plane waves as an effective seismic excitation

The method proposed to handle plane wave propagation analyses in arbitrary complex media is sketched in Figure 1.2. Specifically, GeoELSE has been equipped with a suite of subroutines suitable for the computation of the effective nodal forces from the analytical free-field solution for P-SV-SH plane wave propagation with arbitrary angle of incidence γ through horizontally stratified soil media. The analytical solutions are computed through the Haskell-Thomson (H-T) propagation matrix method (Haskell, 1953; Thomson, 1950). The implementation of these new options was carried out in such a way that the procedure results totally transparent to the users.

The method proposed for plane wave propagation analyses by GeoELSE can be summarized in the following steps:

1. Definition of the input parameters:
 - time dependence of the imposed plane displacement wavefront (it can be either a Ricker wavelet or an arbitrary displacement time history without loss of generality);
 - mechanical properties of the background geological problem (auxiliary problem), assumed to be horizontally layered. Let the vector of layer thickness, soil mass densities, P- and S- wave velocities and quality factors be denoted, respectively, by: H_e , ρ_e , V_P^e , V_S^e and Q_e , with $e = 1, \dots, N_l$, with N_l = total number of layers;
 - plane wave source: type of polarization of seismic input (in-plane, P or SV, or out-of-plane, SH waves);
 - angle of incidence γ (measured clockwise from the vertical, i.e. $\gamma = 0$

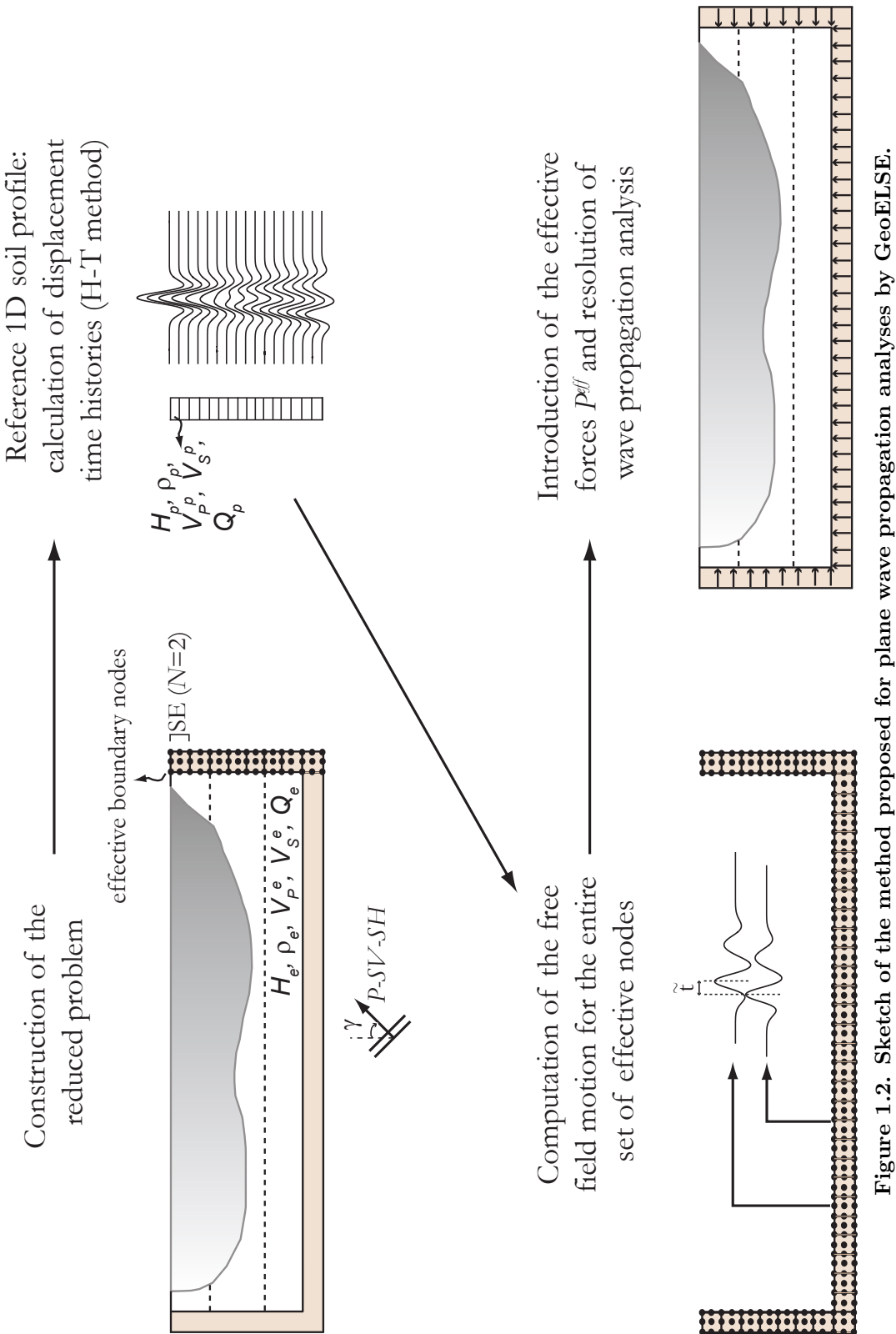


Figure 1.2. Sketch of the method proposed for plane wave propagation analyses by GeoELSE.

stands for vertical plane wave propagation), in- or out-cropping input.

2. Computation of the effective boundary nodes where the effective forces must be applied. A complete list of the LGL nodes is created in descending order with respect to z (depth from the topographical surface).
3. Definition of a reference 1D soil profile: H_p , ρ_p , V_P^p , V_S^p and Q_p with $p = 1, \dots, N_f$, where $N_f \geq N_l$ is the total number of fictitious layers (see Figure 1.2). Each layer is delimited by two adjacent non-coinciding LGL nodes in the z direction. Those nodes located inside the e^{th} layer of the actual geological model (see point 1) have the same properties. Note that nodes with equal z but different x or y coordinates are not duplicated within the soil profile, but only nodes at different depths are considered.
4. Resolution of the Haskell-Thomson (H-T) matrix method for the 1D soil profile determined at previous point. The free-field displacement time histories at the $(N_f + 1)$ interfaces are, hence, computed. Note that the H-T matrix method provides results in the frequency domain, and, thus, a specific convolution process of the analytical transfer function with the imposed displacement time history must be accounted for inside the code.
5. Computation of the free-field displacements at the entire set of effective boundary nodes of the reduced problem. To this end, a proper translation in the time domain is accomplished in order to “distribute” the free-field displacement solution to all spectral nodes where the equivalent seismic excitation must be applied, accounting for any direction of propagation. To explain this, let us recall the solution of the scalar Helmholtz wave equation: $u_0(t - \underline{n} \cdot \underline{r}/V)$ in a 2D space, where $\underline{n} = [n_x \ n_y]$ is the vector normal to the plane wave front, $\underline{r} = [x \ y]$ is the position vector and V is the propagation velocity. It follows that for those nodes located at the same depth (x_k, \bar{y}) the free-field displacement can be calculated as follows:

$$u_0(x_k, \bar{y}; t) = u_0(x_0, \bar{y}; t + \tilde{t}) \quad (1.4a)$$

$$\tilde{t} = \frac{\underline{n}_x \cdot (x_k - x_0)}{V} \quad (1.4b)$$

where x_0 is the reference coordinate with respect to which the temporal shift \tilde{t} is calculated and n_x can be expressed as a function of the angle of incidence γ : $n_x = \sin(\gamma)$. Note that the choice of the reference coordinate depends on the prescribed direction of the incident plane waves.

6. Computation of the effective nodal forces, P^{eff} , based on the free-field displacements obtained at the previous step, and resolution of the wave propagation analysis (reduced model).

As a final remark, note that this method is particularly suitable for the applications that are routinely carried out in engineering practice. Note, in fact,

that a similar approach is used in the finite difference commercial code FLAC (*Fast Lagrangian Analysis of Continua*, www.itascacg.com/software/index.html) for advanced continuum modeling of geotechnical analysis of rock, soil and structural support in 2D and 3D, although it is only applicable to vertical plane waves.

The use of the DRM for simulating plane wave propagation yields different advantages with respect to the conventional approach for plane wave propagation, namely:

- minimization of the spurious reflections due to the absorbing boundary conditions applied on the external boundary of the computational domain. In spite of their effectiveness, the ABCs are not exempt from numerical errors and, thus, non physical reflections from the external boundary towards the localized structure of interest may affect seismic wave propagation in the region under study. In general, absorbing conditions work well for vertical wave incidence ($\gamma = 0^\circ$), while spurious effects tend to increase when γ approaches larger values. Compared to the standard approach (see Section 1.2.1), where non reflecting conditions act on the total wavefield, in the sub-structuring approach boundary conditions on Γ^+ act solely on the diffracted wavefield. As a consequence, the performance of the ABCs is remarkably increased and it is not necessary any more to locate the external boundary far away from the region of interest.
- Natural treatment of non orthogonal incidence to the free surface. In the new version of the code, oblique plane wave propagation analyses can be performed simply by changing the auxiliary problem according to the assumed seismic excitation. Therefore, such an approach results much more flexible for performing parametric analyses with respect to the seismic input.

1.3 VALIDATIONS

The implementation of the code GeoELSE equipped with the DRM for plane wave input has been validated on simple geological configurations to check the accuracy of the numerical results against analytical solutions.

As a first validation of the 2D numerical code, an idealized halfspace subject to the incidence of both vertical ($\gamma = 0^\circ$) and oblique ($\gamma = 10^\circ$ and 20°) plane waves from below has been studied. The temporal dependence of the incident plane wavefront is given by a Ricker wavelet with maximum frequency equal to 2 Hz. Figure 1.3 depicts the reduced model used for the numerical computations by GeoELSE.

The results of this test are illustrated in 1.4: horizontal u_x and vertical u_z displacement time histories obtained along a vertical alignment in the halfspace (denoted by filled triangles in Figure 1.3) for incidence of plane SV (left panel) and P (right panel) waves with angle of incidence $\gamma = 0^\circ$ (top panel), 10° (center panel), and 20° (bottom panel). In each case, the comparison between numerical

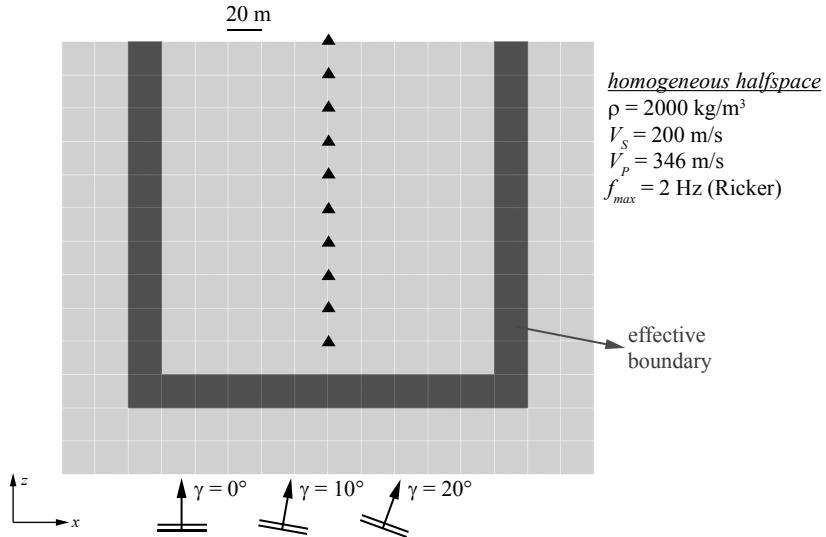


Figure 1.3. 2D reduced model used as validation for plane wave propagation analyses by GeoELSE: homogeneous halfspace subject to both vertical ($\gamma = 0^\circ$) and oblique ($\gamma = 10^\circ$ and 20°) plane waves with temporal dependence given by a Ricker wavelet with $f_{max} = 2$ Hz. The dynamic properties of the homogeneous medium are superimposed on the right hand side of the figure. The effective boundary of the reduced problem is highlighted. The superimposed filled triangles denote the output receivers, where the complete 2D wavefield is calculated.

(black line) and analytical solutions (dashed grey line) turns out to be excellent, being perfectly superimposed. Despite the limited dimension of the reduced numerical model (note that there are only two elements between the effective boundary and the external absorbing boundary), the numerical results do not show any spurious effect due to the ABCs. This is a relevant achievement carried by such an approach for plane wave propagation simulations.

A further validation for the 2D case has been carried out for a geological model consisting of one soft layer ($V_S^1 = 100$ m/s) over halfspace ($V_S^2 = 500$ m/s), as sketched in Figure 1.5. Seismic input is represented by a plane P wave with angle of incidence $\gamma = 0^\circ$ (top panel) and $\gamma = 20^\circ$ (bottom) and with temporal dependence given by a Ricker wavelet with $f_{max} = 2$ Hz.

Figure 1.6 reports the results of this numerical test in terms of horizontal u_x (left hand side) and vertical u_z (right hand side) displacement time histories obtained along a vertical alignment (triangles in Figure 1.5). Even in this case, the comparison between the numerical results obtained by GeoELSE (black line) and the analytical solution (dashed grey line) is very good, although some minor numerical errors are found for oblique wave propagation, probably due to under-sampling effect of the free-field displacement time history. Roughly, for oblique incidence, the time sampling interval of the free-field solution should be: $\Delta t \leq \Delta x_{min}/V_{max}$, where Δx_{min} is the minimum distance between adjacent

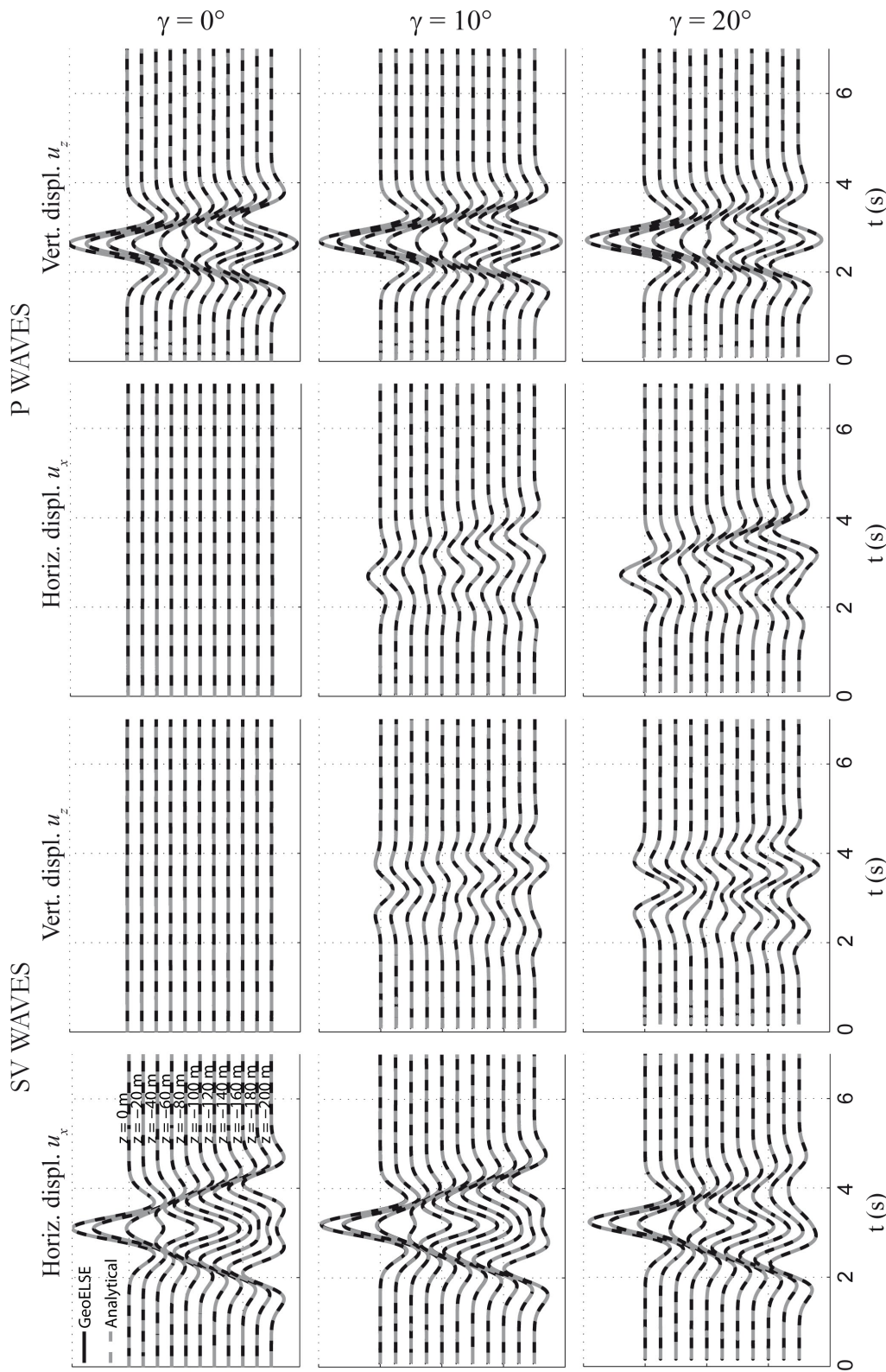


Figure 1.4. Horizontal u_x and vertical u_z displacement time histories along a vertical alignment in the idealized halfspace illustrated in Figure 1.3 (filled triangles): comparison between the numerical results by GeoELSE (black line) and the analytical solution (dashed grey line) for incidence of both SV (left panel) and P (right panel) plane waves with angle of incidence $\gamma = 0^\circ$ (top panel), 10° (center panel), and 20° (bottom panel).

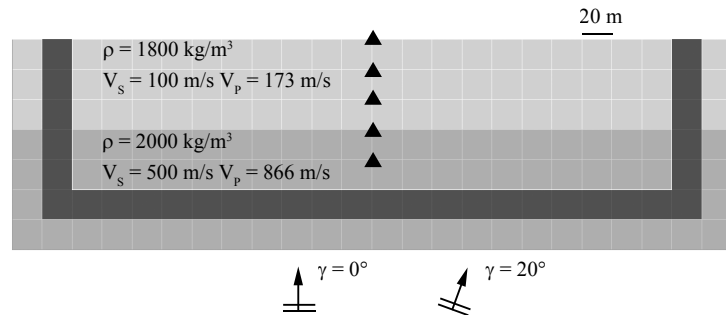


Figure 1.5. 2D geological structure consisting of one soft layer over halfspace: validation of the code for a seismic input represented by plane P waves with angle of incidence $\gamma = 0^\circ$ and $\gamma = 20^\circ$. Input is assumed to be a Ricker wavelet with $f_{max} = 2 \text{ Hz}$. The dynamic properties of the considered materials are superimposed in the graph and the small triangles indicate the output receivers used for validation purposes.

LGL nodes and V_{max} is the maximum propagation velocity.

Making reference to the same test as in Figure 1.6 under vertical propagation of plane P waves, we show in Figure 1.7 the comparison between the results obtained by DRM-based procedure with those computed by the standard single step approach (see Section 1.2.1) at two different sites ($R1$ and $R2$). To have a consistent comparison, the same numerical mesh has been considered for both simulation. It is apparent that the results given by the standard method are badly affected by the spurious reflections coming from the ABCs, especially for those receivers located close to the lateral edges of the computational domain (see $R2$, horizontal component).

As a further validation of the code, Figure 1.8 shows the comparison between the DRM-based method (black line) and the standard single step approach (dashed red line) for the case of a circular soft valley subject to the incidence of vertical ($\gamma=0^\circ$) plane SV waves. The temporal dependence of the plane wavefront is given by a Ricker wavelet with $f_{max}=2 \text{ Hz}$. The results of this test are shown in terms of horizontal displacement time histories (u_x) for a set of equally spaced receivers (superimposed dots) at ground surface. To make the results of the single-step simulation usable as a reference solution, the corresponding numerical grid (not shown here) has been artificially extended in the x direction, for a total length of 2.6 km. This allows, in fact, to minimize the spurious reflection coming from the ABCs.

1.4 ACCOUNTING FOR BI-DIRECTIONAL SEISMIC INPUT

For 2D studies of plane wave propagation in visco-elastic media, the implementation of the DRM in the code GeoELSE takes advantage of the H-T solution for either SV or P input motions, as illustrated in the previous sections. Referring to the 2D case, for simplicity, when both SV and P waves are simultaneously present, a suitable superposition technique should be used to

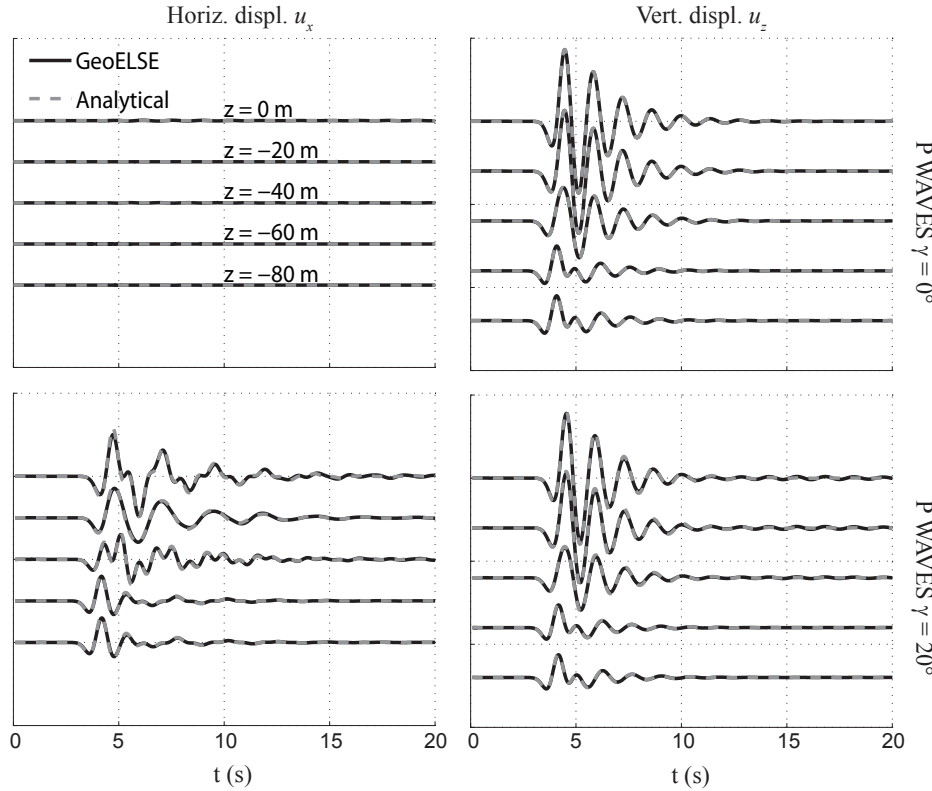


Figure 1.6. Horizontal u_x (left panel) and vertical u_z (right panel) displacement time histories along a vertical alignment for the idealized geological model shown in Figure 1.5: comparison between the numerical results by GeoELSE (black line) and the analytical solution (dashed grey line) for incidence of P plane waves with angle of incidence equal to $\gamma = 0^\circ$ (top panel) and 20° (bottom panel).

take into account the effects of bi-directional seismic input. Since the free-field displacements contributing to the effective boundary forces are given for incidence of plane waves polarized either in SV or P direction independently, the issue is now to set up a suitable approach for reproducing the seismic response of an arbitrary geological model subject to the incidence of multi-directional plane waves. To this end, a suitable convolution process, based on the concept of 2D transfer function matrix (Paolucci, 1999) is proposed. Of course, such a procedure applies only for linear elastic behavior, when the superposition principle applies.

To explain this process, let us denote by u_{SV} and u_P the SV motion polarized in the in-plane direction perpendicular to the direction of wave propagation and the P motion along the direction of wave propagation, respectively. The 2D seismic response at a given observation point k at surface can be expressed by means of the transfer function matrix H_{iW}^k . More specifically, H_{iW} denotes the frequency response along the i^{th} direction (for $i = 1 \dots 2$, Cartesian axes) due to an input harmonic motion of the W type, where W takes the values SV

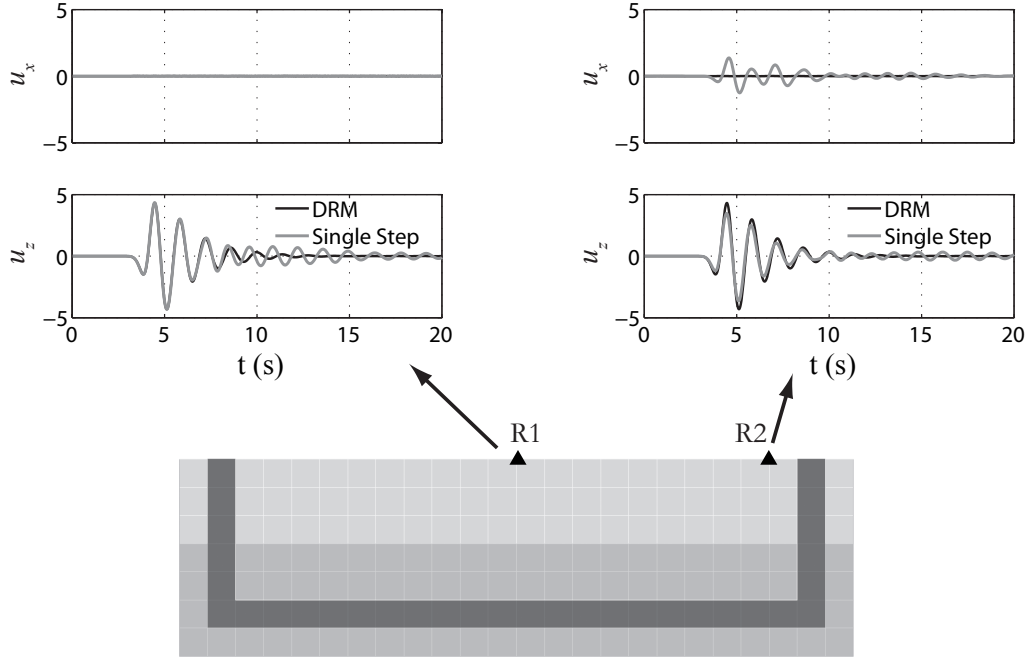


Figure 1.7. Comparison between the DRM-based method (black) and the standard single step approach (grey) for plane wave propagation analyses. The same test as in Figure 1.5 under vertical propagation of plane P waves is considered and the results are provided for two different sites (R_1 and R_2) in terms of displacement horizontal u_x (top panel) and vertical u_z (bottom panel) time histories.

or P.

Such a representation allows one to express the frequency seismic response at a generic site k in a compact form, as follows:

$$\begin{bmatrix} Y_1(f) \\ Y_2(f) \end{bmatrix}^{(k)} = \begin{bmatrix} H_{1SV}(f) & H_{1P}(f) \\ H_{2SV}(f) & H_{2P}(f) \end{bmatrix}^{(k)} \begin{bmatrix} U_{SV}(f) \\ U_P(f) \end{bmatrix} \quad (1.5)$$

where $Y_i(f)$ represents the i^{th} component of ground motion, either in-plane horizontal ($i=1$) or in-plane vertical ($i=2$), and U_W is the reference ground motion of the W type at the reference site. Once each element of the transfer function matrix \mathbf{H} is known at a generic site k , the 2D response of the model can be easily evaluated for any plane wave input motion, if the assumption of linear elastic behaviour holds. In the case of non linear analyses, the input must be given simultaneously along the 2 directions.

Therefore, the following procedure is followed to evaluate the 2D seismic response of arbitrarily complex geological models subject to plane waves with any direction of propagation (see Figure 1.9):

1. construction of the SE mesh for the reduced problem.

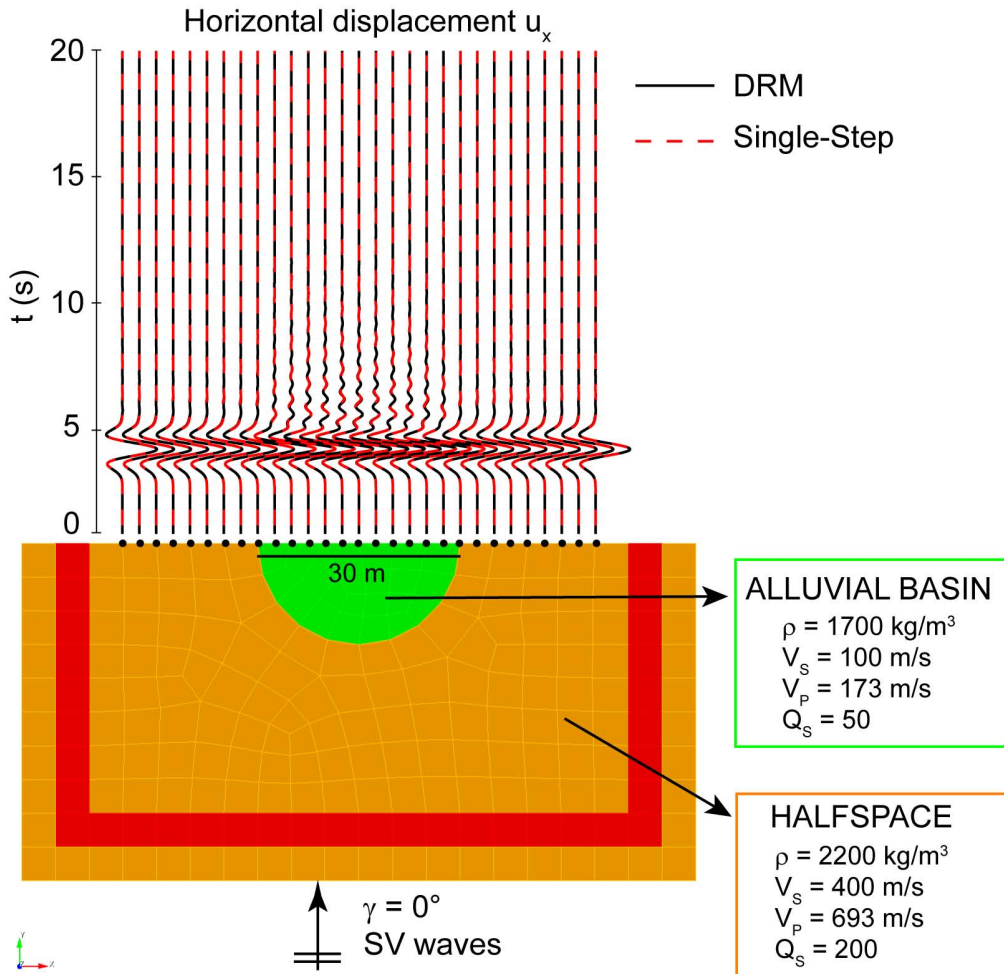


Figure 1.8. Circular valley under vertical plane SV waves: comparison between the DRM-based method (black line) and the standard single step approach (dashed red line) for plane wave propagation analyses, in term of horizontal displacement time histories (u_x). The mechanical properties of the valley and of the surrounding halfspace are superimposed on the graph.

- Two independent numerical analyses by GeoELSE are performed for plane wave propagation polarized in the SV and P direction with angle of incidence γ . At this stage, a Ricker wavelet \hat{u}_W (or any other parametrized wavelet) can be taken into consideration. These analyses are, in fact, needed to compute the 4 components of the transfer function matrix H_{iW} so that any time dependence of input motion can be used.
- From the results obtained by the two numerical simulations at previous point, for a given receiver k , H_{iW}^k is evaluated as the spectral ratio of the Fourier transform of ground motion along the i^{th} direction due to seismic input of the W type (SV or P) over that of input. Referring, for

instance, to the simulation for input motion of the SV type ($W = \text{SV}$), one obtains at a generic site k the three-component response \hat{y}_i^k , for $i = 1, 2, 3$, due to SV plane waves. Hence, the first column of the transfer function matrix in Eq. 1.5 can be computed as the spectral ratio between the Fourier transform of ground motion along the i^{th} direction over that of the prescribed SV input, i.e. $H_{i\text{SV}}^k(f) = F\{\hat{y}_i(t)^k\} / F\{\hat{u}_{\text{SV}}(t)\}$, where F denotes the Fourier transform. The same procedure is applied to calculate the remaining terms H_{iP} by using the results of the simulations under P plane waves.

4. Choice of the reference ground motion u_W .
5. The convolution process, as defined in Eq. 1.5, is carried out. For example, the response along the 1 component, $Y_1(f)$, is computed in the frequency domain as: $\sum_W H_{1W}(f) \cdot U_W(f)$ with $W = \text{SV}$ and P .
6. Finally, the output time histories, either in terms of displacement, velocity or acceleration, can be easily computed by means of the Inverse Fourier transform of $Y_i(f)$, obtained at previous point.

The convolution process has been implemented in a *Matlab* program (see Section 2.5 for further details). The most relevant advantage of this procedure is the possibility of performing parametric analyses with respect to: i) direction of wave propagation; ii) input motions, such as different accelerograms derived from a seismic hazard analysis. Note that, for point ii), only the convolution operations (Eq. 1.5) must be repeated, as the transfer functions H_{iW} have been already evaluated numerically under the assumption of a generic seismic input (e.g. Ricker wavelet).

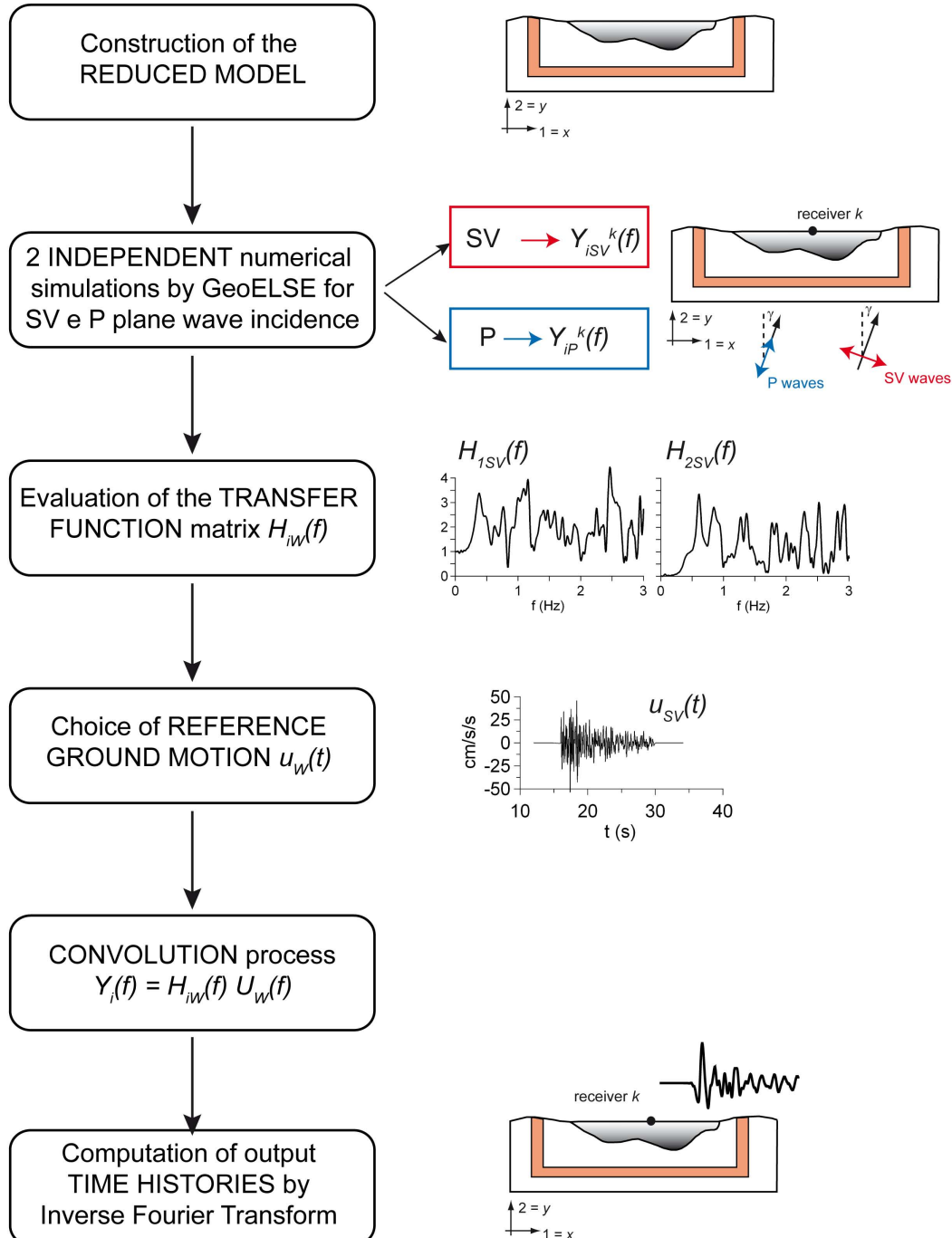


Figure 1.9. Procedure for the evaluation of the seismic response of a localized irregular structure under bi-directional plane wave seismic input. Starting from the reduced problem, discretized by means of spectral elements, two independent numerical analyses are carried out under the incidence of plane SV and P waves with angle of incidence γ . Finally, the seismic response at a generic receiver k is obtained by means of a suitable convolution process in the frequency domain under the assumption of a prescribed time history of seismic input $u_W(t)$.

2. Input files for plane wave propagation analyses

The procedure required for the application of plane wave propagation analyses is shown in Figure 2.1. It can be summarized in four main steps:

1. Generate the SE reduced model making use of the software CUBIT (<http://cubit.sandia.gov/>). Note that the computational grid, provided by a generic file `*.inp`, must include a suitable strip of spectral elements, i.e. the effective DRM boundary, around the irregular structure of interest (e.g. an alluvial basin as sketched in the graph), where the effective forces are applied.
2. Run *GeoELSE2D* with option `SDRM = 3`. This allows one to obtain the coordinates of the LGL node of the effective DRM boundary (files: `lista_macro_coor.txt`, `lista_micro_coor.txt`).
3. Run the interface Matlab program named `plane_4else.m`: file `*.mat` is modified by including the PDRM nodes and FDRM functions in a compatible format for *GeoELSE2D* (step 4).
4. 2D SE simulation by *GeoELSE2D* (option `SDRM = 2`): the displacement time histories at selected sites of the model under study are provided (as output).

2.1 GENERATION OF THE SE MESH WITH CUBIT SOFTWARE

The spatial discretization by quadrilaterals (in 2D) and hexahedral (in 3D) elements of an arbitrarily complex model, honoring the earth's topography and including not only an extended seismic fault but also localized irregular structures, such as alluvial basins or civil engineering elements of various type (viaducts, bridges, underground structures), requires to build up an unstructured mesh of spectral elements. Especially in the 3D case, unstructured tetrahedral meshes, generally used in the Finite Element Method (FEM), can be achieved

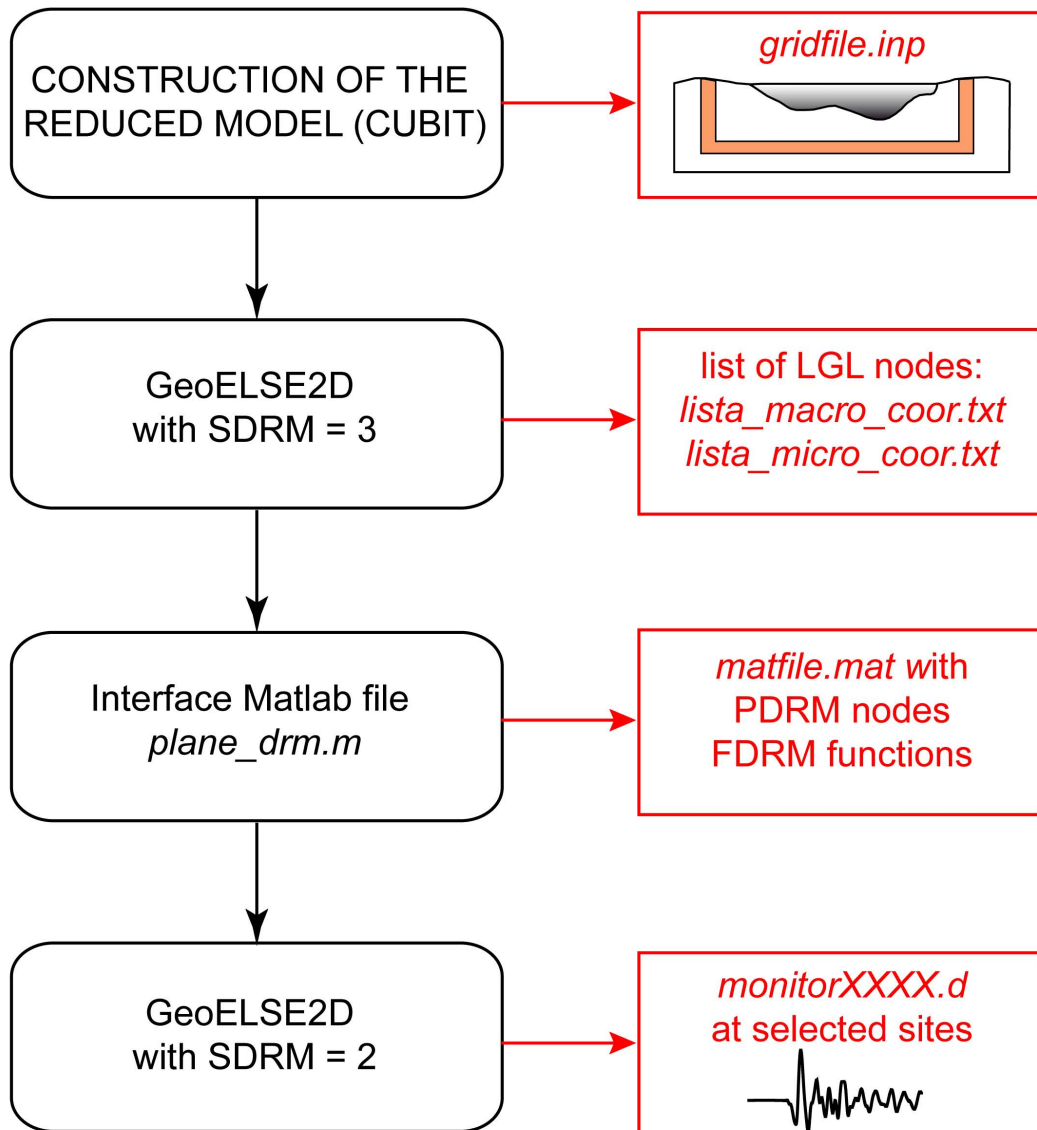


Figure 2.1. Flowchart with the main steps for the application of plane wave propagation analyses (DRM-based approach).

rather easily with commercial or non commercial softwares, while the creation of an unstructured 3D hexahedral grid is still recognized as a demanding and time consuming task.

For the simulations by GeoELSE, the generation of a computational grid is achieved making use of the software CUBIT (<http://cubit.sandia.gov/>), that incorporates a set of powerful and advanced meshing schemes developed to deal with complex unstructured meshing problems. An exhaustive user manual is available at the following link: <http://cubit.sandia.gov/>

[help-version13.0/cubithelp.htm](#).

The basic steps for generating a SE mesh can be summarized as follows:

1. Generate the geometry making use of a CAD based software. NURBS-based 3D modeling tools, such as Rhinoceros software, are preferred.
2. Import the geometry in CUBIT and create the mesh (see following paragraph for some simple criteria for spatial discretization in dynamic applications).
3. Define a set of blocks for the model under study. Each block identifies a homogeneous set of entities (e.g. soil layers, absorbing boundary conditions or DRM boundary elements), where specific features, in terms of soil behaviour, seismic input or absorbing boundary conditions, has to be assigned by the code at run time.
4. Export the mesh to the Exodus II file (*.e). To convert the mesh file from Exodus II (*.e) to ASCII (*.txt) and from ASCII (*.txt) to GeoELSE (*.inp), the filters ncdumps.exe and exo2ucdx_2D.m (exo2ucdx_3D.m in 3D) are used, respectively.

An example of 2D SE mesh generated by CUBIT software is shown in Figure 2.2 for an idealized geological model, with emphasis on the block definition. Once the mesh is built, a set of blocks is defined for the different soil materials (alluvial soft sediments vs. elastic halfspace), for the ABCs applied at the external boundary of the computational domain and for the DRM boundary elements (red strip), as well. Note that, for simplicity, the spectral elements are shown without the inner LGL nodes (they are, in fact, computed at run time). Hereafter this simplified geological model is taken as an illustrative example to describe the application of GeoELSE, coupled with the DRM, for plane wave propagation analyses.

2.1.1 General criteria for spatial discretization

In dynamic applications, criteria for spatial discretization should be kept in mind. The Nyquist theorem provides the maximum spatial sampling step for a proper discretization of the computational grid, based on the minimum number of points to represent the minimum wavelength, equal to 2, so that to avoid

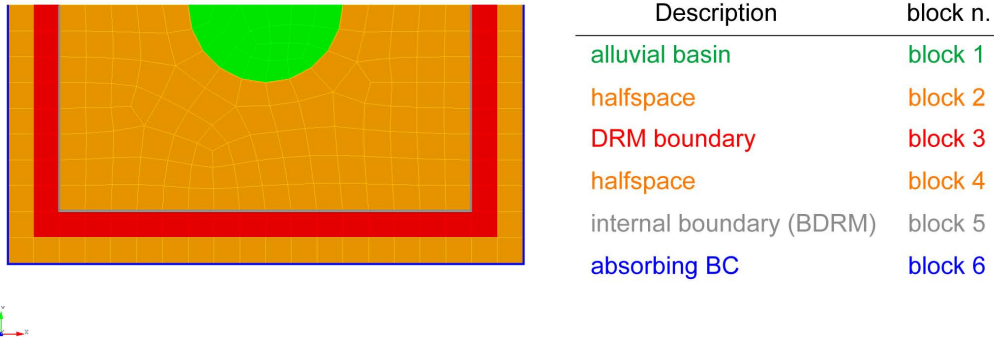


Figure 2.2. Example of 2D spectral element mesh for an idealized geological model, consisting of an alluvial basin in an elastic halfspace. For simplicity, the spectral elements are shown without the inner LGL nodes (computed at run time). A description of the blocks of the model is also provided.

aliasing phenomena:

$$\Delta x \leq \frac{\lambda_{min}}{2} \quad (2.1a)$$

$$\lambda_{min} = \frac{V_{min}}{f_{max}} \quad (2.1b)$$

where Δx is the maximum spatial sampling step, V_{min} is the minimum wave propagation velocity and f_{max} is the maximum frequency to propagate. This is a minimum requirement. However, to get reliable results, Faccioli et al. (1997) showed that, for a homogeneous medium, a mesh should be designed so that there are more than 2.5 points per minimum wavelength, i.e. $G_\lambda \geq 2.5$, while in presence of strong material discontinuities, $G_\lambda \geq 3.5 - 4$ is more appropriate. For sake of comparison, consider that low order FE schemes require generally $G_\lambda \approx 10 - 12$.

Δx in Eq. 2.1 is equal to the spatial step of the mesh for FDs and it is constant. Instead, for SEs this spatial step is not constant, rather it is an average inter-node distance between adjacent LGL nodes. As rule of thumb, for a relatively low spectral degree $N \leq 5$, the characteristic dimension Δl of the spectral element is given roughly by the following expression:

$$\Delta l \leq \frac{\lambda_{min}}{G_\lambda} N \quad (2.2)$$

where N is the degree of the interpolant polynomial and G_λ is taken equal to 4. Therefore, the spatial discretization of the mesh depends on the degree of the interpolant polynomial. This is the main advantage of the method: the accuracy of the problem can be improved either by refining the SE grid (reduce Δl) or by adopting higher SDs (increase N). The latter operation is

completely transparent to the users, who have only to choose the SD , without modifying the mesh, and leaving to the code GeoELSE the task of creating the corresponding LGL nodes and, hence, new degrees of freedom.

2.2 PRELIMINARY ANALYSIS FOR THE COMPUTATION OF THE EFFECTIVE DRM NODES

As a first step, a preliminary analysis has to be performed to obtain the list of coordinates of the LGL nodes that constitute the effective DRM boundary (red strip in Figure 2.2). To this end, the user has to run GeoELSE with the following option: $SDRM = 3$. Output files are:

- *lista_macro_coor.txt*: list of the corner LGL nodes;
- *lista_micro_coor.txt*: list of the remaining (inner) LGL nodes.

Note that these files provides the location of the nodes where the free-field displacement wavefield is computed and, hence, the effective forces are applied.

Input files for GeoELSE are described below:

- *gridfile.inp*: SE mesh. The coordinates of the corner LGL nodes and the grid connectivity are listed.
- *matfile.mat*: data about the material properties and type of seismic input. An example of *.mat file for the simplified example under consideration (Figure 2.2) is illustrated in Figure 2.3.
- *else2_input.d*: with information about the spectral degree and name of input/output files (see Figure 2.4).

2.3 COMPUTATION OF THE EFFECTIVE FORCES: MATLAB INTERFACE PROGRAM

The computation of the displacement wavefield at the DRM boundary nodes can be achieved with the Matlab program named *plane_drm.m*.

The program requires as input the following files:

- *lista_macro_coor.txt* and *lista_micro_coor.txt* (see Section 2.2);

block 1 (basin): $V_s = 100$ m/s, $V_p = 173$ m/s, $\rho = 1700$ kg/m³, $Q = 50$ (f=0.67 Hz)

MATE	1	2	1700	1.7000E+07	1.7000E+07	4.1888E-02
------	---	---	------	------------	------------	------------

block 2 (halfspace): $V_s = 400$ m/s, $V_p = 693$ m/s, $\rho = 2200$ kg/m³, $Q = 200$ (f=0.67 Hz)

MATE	2	2	2200	3.5200E+08	3.5200E+08	1.0472E-02
------	---	---	------	------------	------------	------------

block 3 (DRM): same properties as in block 2

MATE	3	2	2200	3.5200E+08	3.5200E+08	1.0472E-02
------	---	---	------	------------	------------	------------

block 2 (halfspace): $V_s = 400$ m/s, $V_p = 693$ m/s, $\rho = 2200$ kg/m³, $Q = 200$ (f=0.67 Hz)

MATE	4	2	2200	3.5200E+08	3.5200E+08	1.0472E-02
------	---	---	------	------------	------------	------------

ABSO 6 block 6: ABCs

MDRM 3

BDRM 5 block 5: BDRM, internal boundary

SDRM 3

Figure 2.3. Example of *matfile.mat* file for plane wave propagation analysis (GeoELSE simulation with option SDRM = 3).

```
DEGREE 4
GRIDFILE    basin_drm      .inp file
MATFILE     basin_drm      .mat file
OUTFILE     basin_drm_out .out file
```

Figure 2.4. Example of *else2_input.d* file for plane wave propagation analysis (GeoELSE simulation with SDRM = 3).

- *plane.ini* : input parameters for 1D linear visco-elastic seismic wave propagation analyses;
- *matfile.mat*.

Output files are:

- *matfile.mat*, with FDRM and PDRM functions, as required by GeoELSE simulation (step II);

- *LGL_nodes_DRM.txt* : list of LGL effective nodes of DRM boundary;
- *layers_plax.txt* : reference soil profile used for 1D linear visco-elastic analyses;
- *plane.out* : free-field displacement at all soil interfaces of the reference 1D soil profile;
- *pdrm.dat* : list of effective nodes (x,y,z) of DRM boundary;
- *fdrm.dat* : free-field displacement time histories at the effective nodes (t,u_x^0,u_y^0) .

Note that, in the above list, *matfile.mat* is the input file in the format required by GeoELSE simulation with option SDRM = 2 (step II - reduced model).

The core of the analytical procedure implemented in the program *plane_drm.m* is illustrated in 1.2.2. From an algorithmic viewpoint, its main features can be described as follows:

1. interactive definition of the input data regarding the properties of the model under study (*plane.ini* and *matfile.mat*). File *plane.ini* include all the data concerning the input plane wavefront (type of polarization P-SV-SH, angle of incidence, time dependence of input motion), the mechanical properties of the background geological model. Note that the background geological model is assumed to be horizontally layered. A detailed description of file *plane.ini* is given in Table 2.1 and Figure 2.6.
2. Computation of the x,y coordinates of all effective DRM spectral nodes $k = 1, \dots, N^{eff}$ (corner + inner LGL nodes): *LGL_nodes_DRM.txt*. An example is given in Figure 2.5.
3. Construction of a reference 1D soil profile (*layers_plax.txt*): $H_p, \rho_p, V_P^p, V_S^p$ and Q_p with $p = 1, \dots, N_f$, where $N_f \geq N_l$ is the total number of fictitious layers. Each layer is delimited by two adjacent non-coinciding LGL nodes in the y direction (see Figure 2.7).
4. Computation of the free-field displacements at all interfaces of the 1D soil profile (*plane.out*), defined at previous point, from the analytical free-field solution for P-SV-SH plane wave propagation with arbitrary angle of incidence γ through horizontally stratified soil media. The analytical solutions is obtained through the Haskell-Thomson (H-T) matrix method (Haskell, 1953; Thomson, 1950). The matlab program makes uses of the following external functions:
 - *read_acc.m*: reads an external file containing the input time history (*nlin* = number of headerlines to skip; *ncol* = number of columns);

- *HASSH.m*, *HASPSV.m*: calculation of the transfer function at a prescribed interface of the 1D soil profile for SH and P-SV plane wave propagation, respectively.
- *convol.m* : performs convolution of an arbitrary signal with a given transfer function.

The code for the computation of the analytical transfer function under P-SV-SH wave propagation was adapted starting from a previous code (Fortran 77) written by F.J. Sanchez-Sesma (UNAM, Mexico).

5. Calculation of the free-field solution at the entire set of effective boundary nodes. Starting from the displacement time histories computed at all interfaces of the 1D reference soil model, the solution at all effective nodes is obtained by applying a suitable time shift depending on the assumed direction of propagation. For $\gamma = 0^\circ$, time shift is equal to 0 for all nodes.
6. Updating of file *matfile.mat* to include the PDRM (see also *pdrm.dat*) and FDRM (*fdrm.dat*) functions. Note that the total number of PDRM and FDRM function is N^{eff} (number of effective LGL nodes). Figure 2.8 provides an example of *matfile.mat* written after the execution of the code.

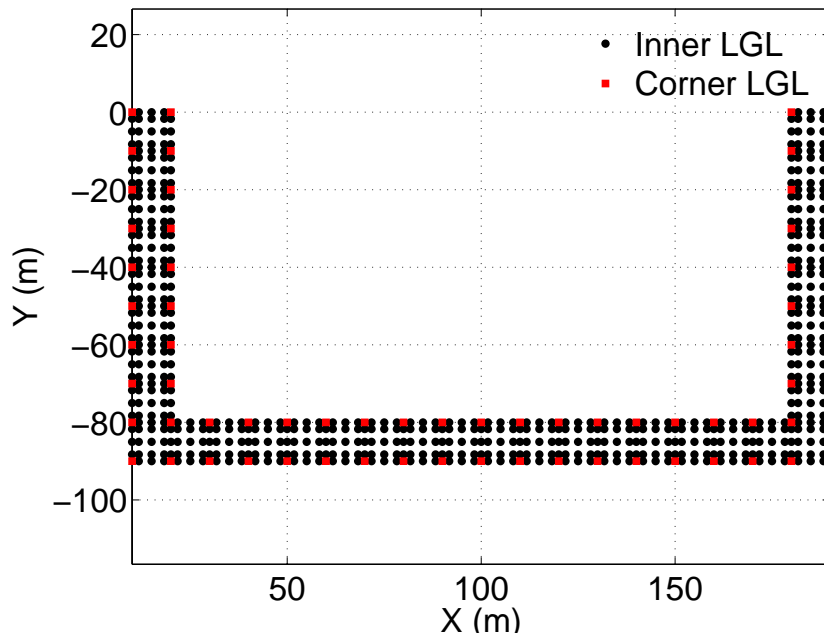


Figure 2.5. Computation of the list of effective DRM nodes. Corner (macro) and inner (micro) LGL nodes are denoted by red squares and black diamonds, respectively.

Table 2.1. Description of file *plane.ini*.

Row 1	1.1 wave type (0=SH,1=P,2=SV) - 1.2 angle of incidence (0° =vertical)
Row 2	2.1 No. of layers N_l
Row 3	3.1 layer no. - 3.2 depth top (m) - 3.3 depth bottom (m) - 3.4 ρ (t/m ³) - 3.5 V_s (m/s) - 3.6 Q_s (-) - 3.7 V_p (m/s) - 3.8 Q_p (-) (Assume $Q_p = Q_s$)
Row 4	4.1 file name of displacement time history
Row 5	5.1 number of rows to skip - 5.2 number of columns - 5.3 time sampling step Δt - 5.4 No. time steps
Row 6	6.1 convolution index (2 if input is outcropping) - 6.2 deconvolution index (1 = conv., 2 = deconv.)

Wave type - Angle of incidence

2.0 0.0

layers of geological model

1

Layer # - Z_{top} (m) - Z_{bottom} (m) - ρ (t/m³) - V_s (m/s) - Q_s - V_p (m/s) - Q_p

1 0.000 -100.000 2.20 400.00 200.00 693.00 200.00

Name of file of time history

ricker.1

rows - # columns - Dt - No. points

0 1 0.01 2001

Conv. index - Deconv. index

1 1

Figure 2.6. Example of file *plane.ini* (see also Table 2.1).

2.4 2D SIMULATION OF REDUCED PROBLEM BY GEOELSE

At this stage, 2D simulation of seismic wave propagation under plane wave propagation can be performed through GeoELSE. The free field displacements (FDRM) at the effective DRM nodes (PDRM), as written in *matfile.mat*, can be now used by GeoELSE to evaluate at run time the effective nodal forces necessary to propagate the target plane wavefront.

Input files for GeoELSE simulation are:

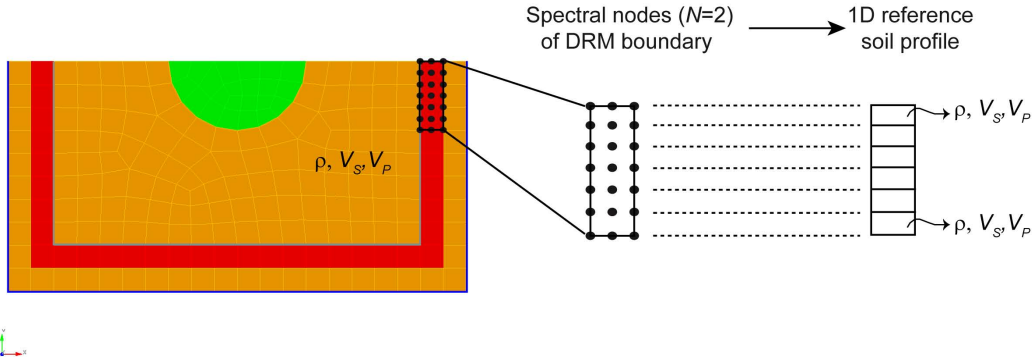


Figure 2.7. Procedure to define a reference 1D soil profile for the computation of the free field solution under plane wave input.

```

.MATE    1      2      1700  1.7000E+07  1.7000E+07  4.1888E-02
.MATE    2      2      2200  3.5200E+08  3.5200E+08  1.0472E-02
.MATE    3      2      2200  3.5200E+08  3.5200E+08  1.0472E-02
.MATE    4      2      2200  3.5200E+08  3.5200E+08  1.0472E-02
.ABSO   6
.iMDRM  3
.BDRM  5
n. effective node
SDRM 2
x (m)          y (m)          scale factor (=1)
.PDRM 1 188.273300 0.000000 1
.t(s)           uxi(m)        uyi(m)
.FDRM 1 50 2001 0.000000e+000 0.000000e+000 0.000000e+000 1.000000e-002 5.644200e-011 0.000i
600000e-001 -7.506893e-011 0.000000e+000 9.700000e-001 7.532698e-011 0.000000e+000 9.80000i
e+000 -5.775660e-009 0.000000e+000 1.930000e+000 -6.762463e-009 0.000000e+000 1.940000e+000
type function
n. time steps
.PDRM 2 185.000000 0.000000 1
.FDRM 2 50 2001 0.000000e+000 0.000000e+000 0.000000e+000 1.000000e-002 5.644200e-011 0.000i
600000e-001 -7.506893e-011 0.000000e+000 9.700000e-001 7.532698e-011 0.000000e+000 9.80000i
e+000 -5.775660e-009 0.000000e+000 1.930000e+000 -6.762463e-009 0.000000e+000 1.940000e+000
.....
total n. of effective nodes (Neff)
.....
.PDRM 685 10.000000 -90.000000 1
.FDRM 685 50 2001 0.000000e+000 0.000000e+000 0.000000e+000 1.000000e-002 -6.529201e-014 0.1
9.600000e-001 6.477621e-014 0.000000e+000 9.700000e-001 -6.557887e-014 0.000000e+000 9.80i

```

The figure shows a matfile.mat file for GeoELSE simulation. It includes header parameters like MATE, ABSO, iMDRM, BDRM, and SDRM. Below this, it defines an effective node (PDRM 1) with coordinates (188.273300, 0.000000) and a scale factor of 1. It then lists time steps (t(s)) and displacement components (u_xⁱ(m), u_yⁱ(m)) for a FDRM entry. The FDRM entry contains complex numbers representing wave parameters. The file continues with more PDRM and FDRM entries, followed by a total number of effective nodes (N^{eff}). The final part of the file shows another PDRM entry with coordinates (10.000000, -90.000000) and a scale factor of 1.

Figure 2.8. Example of matfile.mat for GeoELSE simulation with SDRM = 2 (step II of DRM procedure) for plane wave propagation. This file is written after the execution of the code plane_drm.m.

- gridfile.inp: mesh;
- matfile.mat: output of program *plane_drm.m*;
- else2_input.d: spectral degree, input files, output file, time step, total duration of simulation and list of output receivers.

An example of *else2_input.d* is given in Figure 2.9.

It is worth making some remarks on the choice of the time step Δt for

simulations by GeoELSE. In GeoELSE, the system of equations of motion for all degrees of freedom of the system under study is discretized in time using a finite-difference scheme. In particular, an explicit 2nd order Leap-Frog and 2nd order Backward (LF2-B2) time advancing scheme is adopted. Note that explicit scheme are not unconditionally stable but they must satisfy the well known Courant-Friedrichs-Levy (CFL) condition, that reads as follows:

$$\Delta t \leq v \frac{\Delta x_{min}}{V_{max}} \quad (2.3)$$

where Δx_{min} is the minimum distance between any couple of adjacent LGL nodes, V_{max} is the maximum propagation velocity, and v is a positive constant so that: $0 < v < 1$. The value of this parameter depends on the dynamic properties of the medium under study, in particular, on the Poisson's ratio ν . For $\nu < 0.3$, v assumes values approximately equal to 0.2 (Faccioli et al., 1997). Since Δx_{min} is associated to the nodes close to the element edges, where the grid size scales as N^{-2} , the stability condition becomes prohibitive for large values of spectral degree, for which an implicit time scheme would be recommended.

```

DEGREE 4

GRIDFILE    basin_drm
MATFILE     basin_drm
OUTFILE     basin_drm_out
dis vel acc sts str rot    options for animation
OPTIONOUT   1 0 0 0 0 0 1 2  Option for output files
                           ^

Timestep 0.25e-3      time step Δt (s)

STOPTIME 20          total duration T (s)

TMONITOR 40          time step for output time history (TMONITOR*Δt)

           x (m)      y (m)
MONITOR   30          0
MONITOR   35          0  }
MONITOR   40          0  } set of receivers
...

```

Figure 2.9. Example of `else2_input.d` for GeoELSE simulation with SDRM = 2.

2.5 COMPUTATION OF THE SEISMIC RESPONSE UNDER BI-DIRECTIONAL PLANE WAVES

The procedure illustrated in Section 1.4 has been implemented in a Matlab program: *H2d_convol.m*.

Input files of *H2d_convol.m* are:

- *H2d_convol.ini*: input parameters, as summarized in Table 2.2;
- *monitor.dat*: list of receivers (monitorXXXXX.d files computed by GeoELSE) to be considered in the convolution process;
- *reference.d*: displacement time dependence of ground motion at reference site.
- results of two independent numerical analysis by GeoELSE under P and SV plane waves with arbitrary angle of incidence γ and with time dependence given by a Ricker wavelet (parameters of Ricker wavelet: f_{max} , maximum frequency, and t_0 , time delay. The results of the Ricker analyses under P and SV plane wave propagation should be stored in two directories named <P> and <SV>, respectively.

Execution of program *H2d_convol.m* gives as output the following files:

- *monitorXXXXX_conv2d_ho.d*: horizontal (i.e. along the direction of the cross-section under study) displacement time histories at a given receiver <monitorXXXXX>, as listed in file *monitor.dat*;
- *monitorXXXXX_conv2d_ho.v*: horizontal velocity time histories at receiver <monitorXXXXX>;
- *monitorXXXXX_conv2d_ho.a*: horizontal acceleration time histories at receiver <monitorXXXXX>;
- *monitorXXXXX_conv2d_ho.sa*: horizontal pseudo-acceleration response spectra at receiver <monitorXXXXX>;
- *monitorXXXXX_conv2d_ho.sd*: horizontal displacement response spectra at receiver <monitorXXXXX>;
- *monitorXXXXX_conv2d_up.d*: vertical displacement time histories at receiver <monitorXXXXX>;
- *monitorXXXXX_conv2d_up.v*: vertical velocity time histories at receiver <monitorXXXXX>;

Table 2.2. Description of file *H2d_convol.ini*.

Row 1	1.1 complete path where results of numerical simulations are saved
Row 2	2.1 angle of incidence ($^{\circ}$)
Row 3	3.1 sampling time interval (s) - 3.2 duration (s) of output
Row 4	4.1 sampling time interval (s) - 4.2 scale factor of reference seismogram
Row 5	5.1 sampling time interval (s) - 5.2 scale factor of 2D numerical analyses by GeoELSE (Ricker input)
Row 6	6.1 filename of displacement time history at reference site
Row 7	7.1 maximum frequency f_{max} (Hz) - 7.2 time offset t_0 (s) of Ricker wavelet
Row 8	7.1 logic variable (1/0), choose 1 to band-pass filter output response Filter design: acausal 3rd order Butterworth
Row 9	9.1 minimum cut-off frequency (Hz) - 9.2 maximum cut-off frequency (Hz) of the filter 9.1 and 9.2 are used if 8.1 is equal to 1
Row 10	10.1 logic variable (1/0), choose 1 to compute displacement and acceleration response spectra
Row 11	11.1 logic variable(1/0), choose 1 to write the transfer function matrix at any receiver

- *monitorXXXXX_conv2d_up.a*: vertical acceleration time histories at receiver <*monitorXXXXX*>;
- *monitorXXXXX_conv2d_up.sa*: vertical pseudo-acceleration response spectra at receiver <*monitorXXXXX*>;
- *monitorXXXXX_conv2d_up.sd*: vertical displacement response spectra at receiver <*monitorXXXXX*>;

Note that the above files are saved in the directory <convolution>, created by the program itself.

References

- Bielak, J. and Christiano, P. (1984). On the effective seismic input for non-linear soil-structure interaction systems. *Earthq. Eng. Struct. Dyn.*, 12(1):107–119. [1]
- Bielak, J., Loukakis, K., Hisada, Y., and Yoshimura, C. (2003). Domain reduction method for three-dimensional earthquake modeling in localized regions, part I: Theory. *Bull. Seismol. Soc. Am.*, 93(2):817–824. [1]
- Bielak, J., MacCamy, R. C., McGhee, D. S., and Barry, A. (1991). Unified symmetric BEM-FEM for site effects on ground motion - SH waves. *J. Eng. Mech.*, 117(10):2265–2285. [1]
- Faccioli, E., Maggio, F., Paolucci, R., and Quarteroni, A. (1997). 2D and 3D elastic wave propagation by a pseudo-spectral domain decomposition method. *J. Seism.*, 1(3):237–251. [3, 20, 27]
- Fah, D., Suhadolc, P., Mueller, S., and Panza, G. F. (1994). A hybrid method for the estimation of ground motion in sedimentary basins: Quantitative modeling for Mexico city. *Bull. Seismol. Soc. Am.*, 84(2):383–399. [1]
- Graff, K. F. (1975). Wave motion in elastic solids. Oxford University, New York, Dover Publications. [4]
- Haskell, N. A. (1953). The dispersion of surface waves on multilayered media. *Bull. Seismol. Soc. Am.*, 43(1):17–34. [4, 23]
- Herrera, I. and Bielak, J. (1977). Soil structure interaction as a diffraction problem. In Proceedings VI World conference earthquake engineering, New Delhi, pages 19–24. [1]
- Loukakis, K. (1988). Transient response of shallow-layered valleys for incident SV waves calculated by finite element method. M. Sc. Thesis, Department of Civil Engineering, Carnegie Mellon University, Pittsburgh, Pennsylvania. [1]

Mita, A. and Luco, J. E. (1987). *Dynamic response of embedded foundations: a hybrid approach.* Comp. Meth. Appl. Mech. Eng., 63(3):233–259. [1]

Oprsal, I. and Zahradník, J. (2002). *Three-dimensional finite difference method and hybrid modeling of earthquake ground motion.* J. Geophys. Res., 107(B8):2161–. [1]

Paolucci, R. (1999). *Numerical evaluation of the effect of cross-coupling of different components of ground motion in site response analyses.* Bull. Seismol. Soc. Am., 89(4):877–887. [11]

Thomson, W. T. (1950). *Transmission of elastic waves through a stratified solid medium.* Journal of Applied Physics, 21(2):89–93. [4, 23]

Yoshimura, C., Bielak, J., Hisada, Y., and Fernandez, A. (2003). *Domain Reduction Method for three-dimensional earthquake modeling in localized regions, Part II: Verification and applications.* Bull. Seismol. Soc. Am., 93(2):825–841. [1]

Zahradník, J. and Moczo, P. (1996). *Hybrid seismic modeling based on discrete-wave number and finite-difference methods.* Pure Appl. Geophys., 148(1):21–38. [1]